Bridge-contact microdisk lasers formed by wet chemical etching

© A.A. Obraztsova[1], A.A. Pivovarova[2], S.D. Komarov[1], I.S. Fedosov[1], K.A. Ivanov[1], N.A. Kalyuzhnyy[2], S.A. Mintairov[2], N.D. Il'inskaya[2], Yu.P. Yakovlev[2], I.S. Makhov[1], N.V. Kryzhanovskaya[1], A.E. Zhukov[1]

[1] HSE University,
190121 St. Petersburg, Russia
[2] Ioffe Institute,
191024 St. Petersburg, Russia
E-mail: aobraztsova@hse.ru

Received February 3, 2025
Revised April 10, 2025
Accepted April 17, 2025

This work presents an approach to the fabrication of quantum dot microlasers on GaAs substrates featuring a disk-shaped cavity, a bridge-type electrical contact and a supporting mesa formed by wet chemical etching. The bridge structure consists of two mesa structures connected by a suspended gold beam, one of which is actually a microdisk cavity, and the other allows to create an external electrical contact. The proposed method opens up ways to fabricate small-diameter injection microlasers, as it obviates the need for wire bonding to the top surface of the microlaser cavity. Microlasers with a bridge electrical contact were fabricated, the formation of a close-to-vertical microcavity side-wall in the active region of the structure was demonstrated and the electroluminescence spectra of the microlasers were obtained in a wide range of pump currents, confirming the possibility of lasing both at room and elevated temperatures.

Keywords: microlasers, bridge contact, whispering gallery modes, wet chemical etching.

DOI: 10.61011/SC.2025.01.61073.7587

1. Introduction

Semiconductor whispering gallery mode quantum-dot microdisk lasers are one of the most promising areas in the development of light microemitters that are used in various optoelectronic applications ranging from optical communication systems to biomedical sensing [1,2]. Due to a high Q factor [3], low lasing threshold [4] and lateral direction of output radiation, they have considerable advantages over other types of microlasers (vertically-emitting lasers, photonic crystal lasers, etc.). Efforts have been taken over recent years [5–8] to integrate microdisk lasers with other elements and to finally use them as part of photonic integrated circuits. A reliable electric contact is required for integration of such lasers. Small sizes of microlasers make it difficult to provide electric contact to them through direct soldering (welding) or microprobe contact. Moreover, integrated form of microlasers with photonic integrated circuit requires electric connections to be made between circuit components, which also shall be accomplished in a single process cycle.

This work describes an approach to creating bridge-type microdisc lasers with an outboard bonding pad. Bridge structure consists of two isolated mesa structures with an air metal contact thrown between them. The key feature of this structure is in that the bonding pad is brought out onto a free-standing dielectrically isolated supporting mesa. Air etching under the metal contact provides electric insulation of the heterostructure layers between the mesas [9,10]. Such structural arrangement provides not only stable electric pumping without degrading the functional properties of the microlaser, but is also used to overcome the minimum microlaser size confinement induced by the capabilities of forming a contact with the upper surface of the cavity.

Fabrication of microlasers usually includes synthesis by molecular beam or vapor phase epitaxy methods followed by the formation of microcavities in the form of a disk or ring using photo or electron-beam lithography and etching. To form microdisc cavities with outboard contact, this work uses a wet chemical etching method that, compared with plasma-enhanced chemical etching, doesn't require additional planarizing coatings to form the bridge electric contact between the microlaser and bonding pad; such coatings deteriorate heat removal and reduce the optical output power due to absorption of the laterally outgoing light [11]. Moreover, in case of wet chemical etching, the bridge contact is formed in a single cycle with mesa etching, because wet etching may be performed laterally under the metal region. At the same time, optimization of wet etching conditions is required to form a vertical-wall mesa.

This work first created microdisk lasers with a bridge contact, demonstrated the formation of a near-vertical microcavity wall near the active region of the structure and achieved lasing at room and higher temperatures.

2. Materials and methods

Laser heterostructure was synthesized by gas-phase epitaxy from organometallic compounds on a n^+-GaAs substrate nonoriented at 6° relative to the (100) plane.

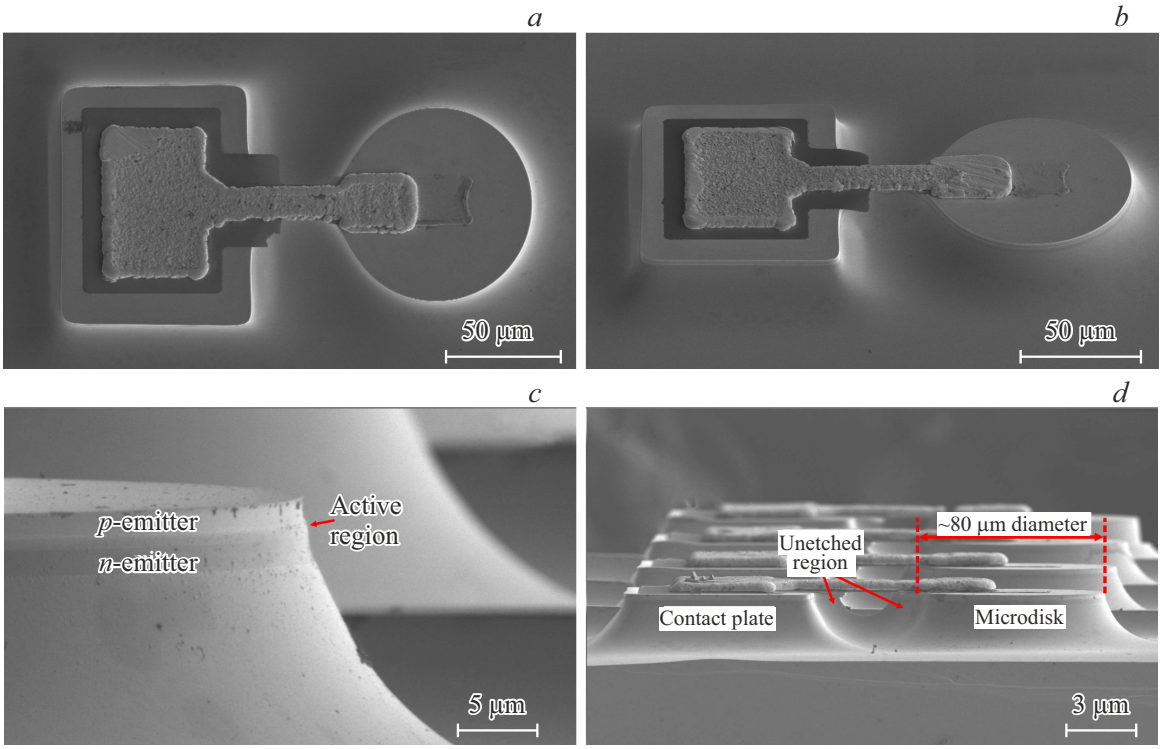

Figure 1. SEM images of formed microlasers with a bridge contact: *a* — plan view, *b* — angle view, *c* — view of the side wall for deep etching, *d* — view of the devices and unetched region.

The structure consisted of a n^+-GaAs buffer layer, 1.5 μm n-$Al_{0.39}Ga_{0.61}As$ lower emitter layer, 0.75 μm undoped GaAs waveguide layer, 1.2 μm p-AlGaAs upper emitter layer and 0.15 μm p^{++}-GaAs contact layer. The waveguide layer contained an active region consisting of 6 InGaAs/GaAs quantum dot layers that were formed by the deposition of a 2 nm $In_{0.4}Ga_{0.6}As$ layer on GaAs. The quantum dot layers were separated by a 40 nm GaAs spacer.

Microlasers were formed using standard photolithography methods. The lift-off lithography method was used to form dielectric and metallic layers. To isolate the bonding pad from the supporting mesa, a dielectric liner consisting of a two-component TiO_2-SiO_2 system was formed using the magnetron sputtering method. Ohmic contact was formed by the high-vacuum thermal evaporation method with sputtering of the Ag-Mn-Ni-Au system to the p-GaAs and Au-Ge-Ni-Au layer for n-GaAs followed by simultaneous hydrogen burning-in. The ohmic contact was also brought out onto the supporting mesa by the thermal evaporation method, for this Cr-Au sputtering was performed. The resulting metal beam was thickened using selective gold electroplating to a thickness of $\sim 3\,\mu$m.

Mesastructures were etched in a polishing $HBr:K_2Cr_2O_7$ etchant that had similar etching rates for the heterostructure layers, due to which a sufficiently smooth side wall of the mesa was made. Etching was performed to a nominal depth of 20 μm or 23 μm. Etching depth was measured using the Bruker DektakXT stylus profiler. Diameter of the fabricated microdisk lasers was ~ 84 and 80 μm for etching to a depth of 20 μm and 23 μm, respectively, due to lateral etching. Images of the produced structures made using a scanning electron microscope (SEM) are shown in Figure 1. As shown in Figure 1, *c*, slope of the cavity wall near the active region of the heterostructure is almost vertical. However, Figure 1, *d* shows that the heterostructure is underetched in a region under the bridge due to a limited access for the chemical etchant. As a result, a protrusion is formed in the bridge region both on the outboard bonding pad side and microlaser side; the larger the etching depth the smaller the protrusion is. Such protrusion may reduce the Q-factor (increase optical loss) of the laser cavity and, consequently, affect its threshold and spectral properties.

For measurements, a wafer with the formed devices was soldered with the n-contact downward to a copper heat sink that also served as one of the electric contacts and was placed on a solid holder that made it possible to vary the heat sink temperature by means of a built-in two-stage thermal cell and thermal sensor. Electric contact to the outboard bonding pad of the studied microlaser was made using a metallic microprobe. The microlasers were energized by current pulses with a duration of 500 ns and a repetition rate of 4 kHz. Microlaser light was collected by the Mitutoyo MPlan APO NIR 20x microlens and then sent to the Yokogawa AQ6370D optical spectrum analyzer via a multimode optical fiber.

3. Findings

Figure 2, *a* shows electroluminescence spectra of a microdisk laser formed by etching to a depth of 23 μm measured at room temperature for different pumping currents. At low pumping currents, the electroluminescence spectrum of the microlaser corresponds to spontaneous radiation of the InGaAs/GaAs quantum dots [12]. Spectral position of the spontaneous radiation intensity peak corresponds to the basic non-equilibrium carrier junction at the dots and is at $\sim$ 1077 nm. As the pumping current increases, a series of narrow lines corresponding to the whispering gallery modes supported by the microcavity occurs in the long-wavelength area of the spontaneous radiation band. A threshold form of dependence of the integral laser luminescence intensity on pumping current is also a sign of transition into the lasing condition (Figure 2, *b*). Lasing threshold current I_{th} for this microdisk laser is $\sim$ 93 mA, which corresponds to the threshold current density ~ 1.8 kA/cm^2. The microdisk laser demonstrates multimode lasing throughout the studied pumping current range.

Microlasers formed by etching to a smaller depth (20 μm) demonstrate much worse properties than microlasers formed by etching to a depth of 23 μm. As shown in Figure 3, *a*, an increase in the etching depth from 20 μm to 23 μm reduces the threshold laser lasing current multifold. This is most probably caused by a smaller protrusion formed under the bridge contact and, consequently, by lower photon loss due to light scattering for cavities with a larger etching depth. A considerable threshold current growth was actually observed in microring lasers, when a radial waveguide was connected to them, and was associated with the growth of photon loss due to significant light scattering in corners at the interface between the microring cavity and radial optical waveguide [13]. Moreover, microlasers made by large-depth etching demonstrate lasing in a longer-wavelength portion of spectrum notwithstanding that all them are formed from the same epitaxial laser heterostructure. It is known that the growth of loss in quantum-dot lasers leads to a short-wavelength shift of laser generation wavelength [14], which also indicates a lower level of loss in microlasers made by etching to a depth of 23 μm.

The magnitude of full photon loss inherent with the studied microlasers formed with various etching depth may be determined by comparing the generation wavelength at the threshold in microdisks and stripe lasers with different lengths made from the same epitaxial structure. In this case, we also use the fact that the optical confinement factor (both vertical and lateral) is the same for laser modes in both cases. The obtained correlation between the threshold gain and lasing wavelength for stripes with different lengths is shown in Figure 3, *b* assuming that the reflectivity of stripe laser mirrors is equal to 30 %. The level of internal loss of 2 cm^{-1} derived from the dependence of inverse differential quantum efficiency on the cavity length of the stripe-geometry laser was considered. Since microdisk and stripe-geometry lasers are made from the same epitaxial

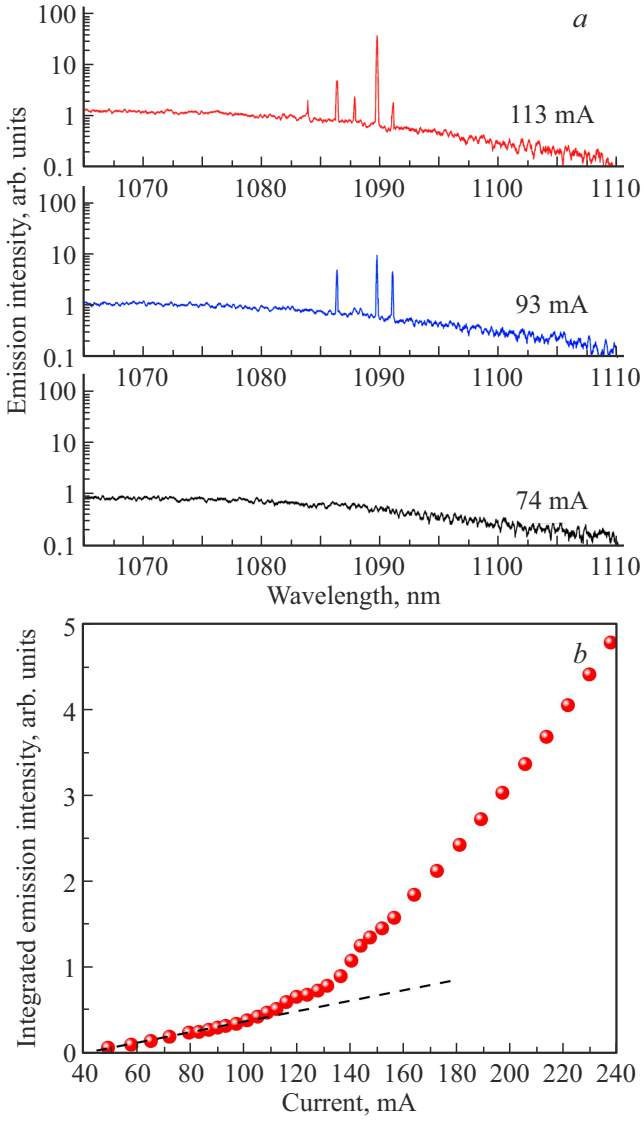

Figure 2. Electroluminescence spectra (*a*) measured at different pumping currents and dependence of the integral electroluminescence intensity on the pumping current (*b*) for the microdisk laser with a nominal etching depth of 23 μm.

wafer, the similar wavelength at the generation threshold is indicative of a similar level of loss in lasers. Then for microdisks with an etching depth of 23 μm, the total optical loss amounts to approximately 20 cm^{-1}, which is consistent with previous reports for microdisks made using plasma-enhanced chemical etching [15]. Microdisk etching to a smaller depth (20 μm) results in significantly higher total optical losses of approximately 55 cm^{-1}.

The next stage addressed spectral and threshold properties The subsequent stage of the study focused on the spectral and threshold characteristics of the microdisk laser formed by etching to a depth of 23 μm at different temperatures (20–90 °C). Growth of the lattice temperature leads to the growth of threshold lasing current (Figure 4, *a*), that is described by the characteristic temperature $T_0 = 45$ K in the

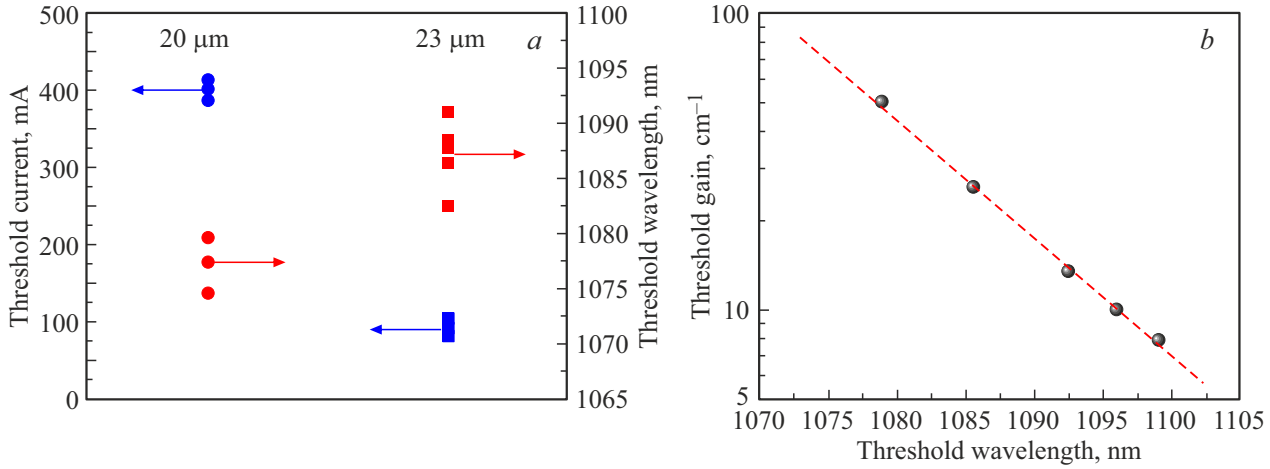

Figure 3. Lasing threshold currents (blue symbols) and wavelength of dominant lasing mode, obtained at the threshold, (red symbols) for the microdisks with etching to a depth of 23 μm (boxes) and 20 μm (dots) (a). Dependence of the threshold modal gain on the lasing wavelength for stripe lasers made from the same epitaxial structure (b).

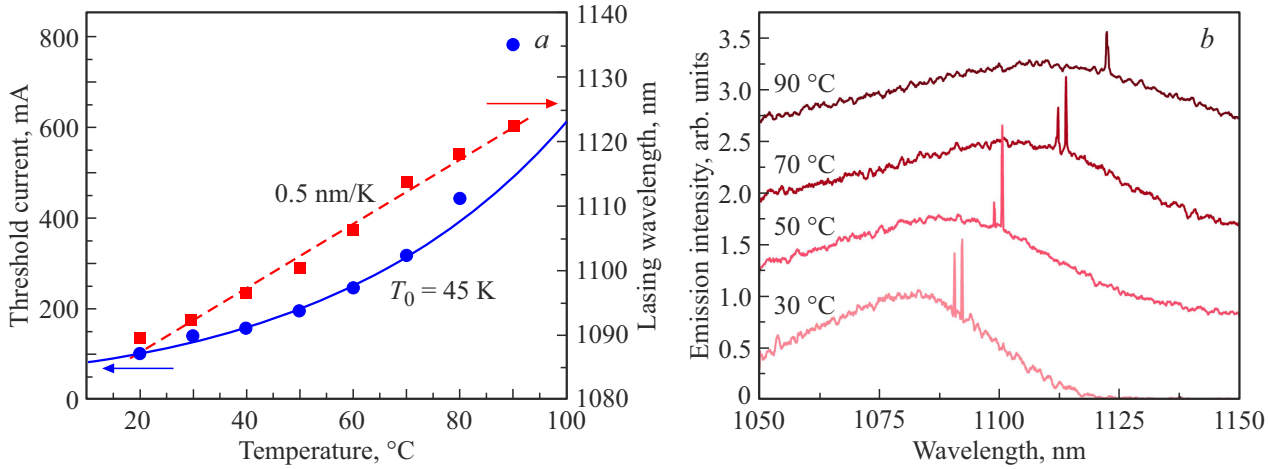

Figure 4. Dependences of the threshold current (dots — experiment, solid line — approximation with the characteristic temperature T_0) and dominating laser mode wavelength (boxes — experiment, dashed line — linear approximation) on temperature (a) and electroluminescence spectra measured at different temperatures with the pumping current equal to $1.15 \times I_{th}$ (b) for the microlaser with an etching depth of 23 μm.

temperature range from 20 °C to 70 °. Laser emission was sustained up to a temperature of 90 °C. Temperature growth of the nonradiative recombination contribution and growth of thermal smearing of charge carrier distribution over the quantum dot states (ground, excited) also increasing the probability of carrier escape from the quantum dots from quantum dots are supposed to be the main reasons of the threshold current growth with temperature.

Temperature growth also leads to a red shift of laser generation wavelength with a characteristic coefficient of ~ 0.5 nm/K (Figure 4, a). A long-wavelength shift of the laser line with temperature may be induced by several main contributions. The first contribution is associated with the variation of the refractive index of the active region of laser with the temperature growth governed by a thermo-optic coefficient of approximately 80 nm/K in microlasers with similar active region [16,17]. The second contribution is extremely weak and is associated with linear thermal expansion of materials forming the microlaser. The third contribution is associated with the long-wavelength shift of the gain spectrum itself with the temperature growth induced by the temperature variation of the band gap of materials forming the active region of the microlaser. Actually, an evident shift of the spontaneous luminescence band of microlasers (Figure 4, b) by ~ 0.45 nm/K is observed as the temperature grows. Therefore, the observed redshift of the lasing wavelength with increasing temperature with a coefficient of 0.5 nm/K that is displayed in this case is caused by a combination of all above-mentioned factors, among which band gap narrowing is predominant.

4. Conclusion

This work shows a new approach to creating quantum-dot microdisk lasers based on wet chemical etching and an externally positioned bonding pad. The proposed method makes it possible to eliminate the need for electrical wire bonding to the top surface of the microcavity and, thus, offers the opportunity to make small-diameter injection microlasers. Electroluminescence spectra were obtained to confirm the possibility of multi-mode lasing at various pumping currents. Outboard contacts improve the electric connection stability through the use of soldering or welding for small-diameter lasers and, according to the performed studies, maintain stable operation at elevated temperatures making the proposed technique promising for integration into photonic circuits and optoelectronic devices.

Funding

This study was supported by the grant issued by the Russian Science Foundation No. 22-72-10002, https://rscf.ru/project/22-72-10002/.

Acknowledgments

The work was carried out on the large-scale research facility „Complex optoelectronic stand“ of the HSE Univetsity.

Conflict of interest

The authors declare no conflict of interest.

References

[1] Y.C. Chen, X. Fan. Adv. Opt. Mater., **7** (17), 1900377 (2019).
[2] A.I. Nosich, E.I. Smotrova, S.V. Boriskina, T.M. Benson, P. Sewell. Optical Quant. Electron., **39**, 1253 (2007).
[3] L. He, Ş.K. Özdemir, L. Yang. Laser Photon. Rev., **7** (1), 60 (2013).
[4] X.F. Jiang, C.L. Zou, L. Wang, Q. Gong, Y.-F. Xiao. Laser Photon. Rev., **10** (1), 40 (2016).
[5] E. Stock, F. Albert, C. Hopfmann, M. Lermer, C. Schneider, S. Höfling, A. Forchel, M. Kamp, S. Reitzenstein. Advanced Mater., **25** (5), 707 (2013).
[6] Y. Wan, D. Jung, D. Inoue, J.C. Norman, C. Shang, A.C. Cossard, J.E. Bowers. *2018 Progress in Electromagnetics Research Symp.* (Toyama, Japan, 2018) p. 249.
[7] N.V. Kryzhanovskaya, F.I. Zubov, E.I. Moiseev, A.S. Dragunova, K.A. Ivanov, M.V. Maximov, N.A. Kalyuzhnyy, S.A. Mintairov, S.V. Mikushev, M.M. Kulagina, J.A. Guseva, A.I. Likhachev, A.E. Zhukov. Laser Phys. Lett., **19** (1), 016201 (2021).
[8] N.V. Kryzhanovskaya, K.A. Ivanov, N.A. Fominykh, S.D. Komarov, I.S. Makhov, E.I. Moiseev, J.A. Guseva, M.M. Kulagina, S.A. Mintairov, N.A. Kalyuzhnyy, A.I. Lihachev, R.A. Khabibullin, R.R. Galiev, A.Yu. Pavlov, K.N. Tomosh, M.V. Maximov, A.E. Zhukov. J. Appl. Phys., **134**, 103101 (2023).
[9] N.D. Ilinskaya, A,A. Pivovarova, E.V. Kunitsyna, Yu.P. Yakovlev. Patent 2783353 RU (Russia, 2022).
[10] A.A. Pivovarova, E.V. Kunitsyna, G.G. Konovalov, S.O. Slipchenko, A.A. Podoskin, I.A. Andreev, N.A. Pikhtin, N.D. Ilisnakaya, Yu.P. Yakovlev. ZhPS, **90**(1), 102 (2023). (in Russian).
[11] N.V. Kryzhanovskaya, E.I. Moiseev, F.I. Zubov, A.M. Mozharov, M.V. Maximov, N.A. Kalyuzhnyy, S.A. Mintairov, M.M. Kulagina, S.A. Blokhin, K.E. Kudryavtsev, A.N. Yablonskiy, S.V. Morozov, Yu. Berdnikov, S. Rouvimov, A.E. Zhukov. Photon. Res., **7** (6), 664 (2019).
[12] M.V. Maximov, A.M. Nadtochiy, S.A. Mintairov, N.A. Kalyuzhnyy, N.V. Kryzhanovskaya, E.I. Moiseev, N.Yu. Gordeev, Yu.M. Shernyakov, A.S. Payusov, F.I. Zubov, V.N. Nevedomskiy, S.S. Rouvimov, A.E. Zhukov. Appl. Sci., **10**, 1038 (2020).
[13] N.A. Fominykh, F.I. Zubov, K.A. Ivanov, E.I. Moiseev, A.M. Nadtochiy, S.A. Mintairov, N.A. Kalyuzhnyy, I.A. Melnichenko, V.V. Pirogov, S.A. Scherbak, B.D. Urmanov, A.V. Nahorny, N.V. Kryzhanovskaya, A.E. Zhukov. St. Petersburg Polytechnical University. J. Phys. Math., **16** (1.2), 126 (2023).
[14] N.V. Kryzhanovskaya, I.S. Makhov, A.M. Nadtochii, K.A. Ivanov, E.I. Moiseev, I.A. Melnichenko, S.D. Komarov, S.A. Mintairov, N.A. Kalyuzhny, M.V. Maksimov, Yu.M. Shernyakov, A.E. Zhukov. Pisma ZhTF, **50** (21), 57 (2024). (in Russian).
[15] A.E. Zhukov, E.I. Moiseev, A.M. Nadtochiy, N.A. Fominykh, K.A. Ivanov, I.S. Makhov, M.V. Maximov, F.I. Zubov, V.G. Dubrovskii, S.A. Mintairov, N.A. Kalyuzhnyy, N.Yu. Gordeev, Yu.M. Shernyakov, N.V. Kryzhanovskaya. IEEE J. Quant. Electron., **59** (1), 2000108 (2023).
[16] I. Makhov, S. Komarov, N. Fominykh, A. Obraztsova, V. Voitovich, N. Derkach, I. Melnichenko, N. Shandyba, N. Chernenko, M. Solodovnik, A. Lipovskii, Yu. Shernyakov, N. Kalyuzhnyy, S. Mintairov, N. Kryzhanovskaya, A. Zhukov. Optics Lett., **50** (2), 387 (2025).
[17] I. Makhov, K. Ivanov, E. Moiseev, N. Fominykh, A. Dragunova, N. Kryzhanovskaya, A. Zhukov. Nanomaterials, **13**, 877 (2023).

Translated by E.Ilinskaya